TRANSIENT EXCITATION AND DATA PROCESSING TECHNIQUES EMPLOYING THE FAST FOURIER TRANSFORM FOR AEROELASTIC TESTING

W. P. Jennings, N. L. Olsen, and M. J. Walter

Boeing Commercial Airplane Company

SUMMARY

This paper presents the development of testing techniques useful in airplane ground resonance testing, wind tunnel aeroelastic model testing, and airplane flight flutter testing. Included is the consideration of impulsive excitation, steady-state sinusoidal excitation, and random and pseudorandom excitation. Reasons for the selection of fast sine sweeps for transient excitation are given.

The use of the Fast Fourier Transform Dynamic Analyzer (HP-5451B) is presented, together with a curve fitting data process in the Laplace domain to experimentally evaluate values of generalized mass, modal frequencies, dampings, and mode shapes. The effects of poor signal-to-noise ratios due to turbulence creating data variance are discussed. Data manipulation techniques used to overcome variance problems are also included.

The experience is described that was gained by using these techniques since the early stages of the SST program. Data measured during 747 flight flutter tests, and SST, YC-14, and 727 empennage flutter model tests are included.

INTRODUCTION

In choosing a test method to approach an airplane flight flutter test, the implied ground rules, composed of flight safety, historical constraints, available equipment, test costs, test time, original or derivative model, etc., usually have a large impact on the procedures ultimately used. Until recently, flight flutter tests at Boeing used two forms of excitation; impulsive and slow swept sine wave (steady-state response).

Transient testing techniques have been employed from the earliest times in the form of impulsive testing such as control surface kicks to excite aircraft during flutter tests. Modal frequency and damping have generally been determined by evaluating the logarithmic decrement of a decaying response signal. Hand analyses in the time domain of control surface kick responses are limited to those modes which fall within the bandpass of the control surface; i.e., as long as the assumption that the forcing function was effectively a unit impulse or delta function over the frequency range of interest, a transfer function can be inferred by analyzing the response. The log decrement manual analysis of the response time history can yield excellent results if there is a single mode of interest and the frequency-damping product of that mode is small relative to that of the other modes. Also, the eigenvector for that mode at the spacial point of measurement must be of the same relative scale

as adjacent modes. If there are several modes with roughly equal vectors having similar frequency-damping products, it becomes extremely difficult, if not impossible, to obtain meaningful damping information. The differences in the frequencies of the two modes can be obtained from the beat frequency, but the damping of either mode is difficult to evaluate using the log decrement method. These anomalies in the past generated the requirements to obtain swept frequency (steady-state response) measurements.

These steady-state techniques, coupled with the use of Kennedy-Pancu's vector plot method (ref. 1), provided a means of identifying and tracking the frequencies and dampings of vibration modes during flutter test programs. As usual, this increased the understanding of the dynamics of the system but required a considerable increase in flight test time over that previously used for control surface kicks.

In 1969, a small improvement in swept sine test times was achieved through the use of pseudosteady-state methods and a vector-plotting analysis system (refs. 2 and 3). This system produced results with the structure reaching approximately 90% of steady-state response and was based on the principle that the damping in a system is directly proportional to the number of cycles of oscillation for a given vector phase swing when sweeping through a resonance using a sweep rate $\dot{\omega} = R\omega^2$ (refs. 3 and 4). This method gave reasonable insight into the damping of the modes and approximate modal frequencies; however, the test time required was still too long for the method to be used more than sparingly.

In late 1969, transform methods using the Fast Fourier Transform began to appear practical on digital machines. Experiments into their use were initiated (ref. 5), reevaluating all forms of excitation.

TRANSFORM METHODS

Impulse Excitations

Initial experiments were based upon impulsive excitations; i.e., band-limited delta functions obtained from exponential decaying time domain forcing functions. The initial choice of this function was based upon the idea that if the forcing function could be assumed to be a delta function (over the frequency range of interest), then only the response would have to be transformed, thus, saving on-line computational time. Using this forcing function to excite a multiple degree-of-freedom system presents some problems. As the bandwidth of the pulse increases, the time duration has to decrease; if the peak force remains the same, the total energy has to decrease. Signal-to-noise ratios soon become the most significant consideration. Increasing the peak force to gain some energy soon results in concern because nonlinearities result from local structural deformations. Using a peak force level that avoids questions of nonlinearities with sufficient bandwidth to excite the principal modes will usually result in the response signal being significantly influenced by background noise from acoustical, mechanical, and electrical sources. In the case of flight flutter tests, the atmospheric turbulence can impart more energy than the controlled excitation source.

Considering other waveforms, such as rectangular, trapezoidal, or sin (X)/X time histories, results in small gains in available energy over their effective bandwidths if the comparison is performed with equal peak force and equivalent bandwidth. These small gains are of little significance when orders of magnitude are needed to overcome signal-to-noise ratio problems. The sensitivity to noise using transform methods is the penalty paid for obtaining considerably less time domain data.

Nonimpulse Excitations

Forcing functions that can be employed to overcome signal-to-noise ratio problems are random, pseudorandom, and fast sine sweeps. Random excitation can be considered from two points of view. Since atmospheric turbulence exists, it may be taken advantage of, and the resulting response signal can be processed. To do so requires assumptions to be made about the spectrum of the atmospheric turbulence forcing function. Since this forcing function is a global source of energy to the airplane in flight, it does not lend itself to measurement or analysis, so the assumption must be made that the amplitude spectrum has to be flat or at least well behaved in that it contains no zeros in the frequency band of interest. If airplane response measurements are made during the time a wave front (such as a step function) is being penetrated by the vehicle, then another problem exists due to the time delays as the wave front imparts energy to the airplane. These time delays can cause the energy stored in the vehicle to be reinforced or cancelled as the input energy propagates along the airplane. To approach the problem by recording many independent time histories to enable performing power spectral densities with large degrees of freedom brings back the disadvantages of steady-state sine wave techniques—too much measurement time is consumed making the analysis. If power spectral density (PSD) analysis is performed, then no assumption need be made as to the phase spectrum of the excitation. The disadvantage is that no phase information is contained in the resultant PSD. This makes the problem of system identification more difficult when several modes are overlapping. The Hilbert transform can be used to obtain phase information from the PSD. However, the assumption of minimum phase must be made. Minimum phase indicates no zeros in the right hand Laplace (s) domain.

Assumptions leave targets for stones to be thrown at, independent of whether the assumptions are correct. Therefore, the best approach might be the use of analysis techniques employing minimum assumptions.

The approach of actually measuring the causal relationship between some known input (force) and an output (acceleration) would seem the optimum. In this method, the coherence function is also available as a measure of the causal relationship between input and output. An alternate approach is to use random excitation, hopefully uncorrelated with the turbulence source, to excite the airplane. One problem with the random excitation approach is that if both the random forcing function along with some response signal is measured so that the transfer function can be calculated, the problem of leakage in the frequency domain has to be dealt with. Prior to Fourier transforming the data, some window function (such as Hanning) has to be applied to the time domain data to minimize leakage. The window can effectively reduce the leakage problem; however, the transfer function needs to be corrected for the effects of the particular window used. This is not a straight forward correction, since the window affects both the apparent frequency and the damping, and it is frequency dependent.

If the forcing function is chosen to be a periodic time domain signal, then windowing and the associated problems are eliminated. Both pseudorandom and the fast sine can fall in this category. Of these two forcing functions, the sine sweep has provided better results when systems that exhibit nonlinearities such as a stiffening spring are encounted. This form of excitation has assisted in the understanding of such nonlinear effects. Some insight might come from a look at the amplitude probability distributions of these functions. Another factor favoring the fast sine sweep is that the signal-to-noise ratios of the response signal are improved. Using the fast sine sweep, a given mode will reach a higher percentage of its steady-state response compared with random excitation, especially when systems are lightly damped.

In some systems, limits are imposed on the peak force that can be used. More energy can be imparted to the specimen using the fast sine sweep in these systems. If the 3σ peaks of the random

signal are kept at the same peak value of the fast sine sweep, more energy is available from the fast sine sweep to improve signal-to-noise ratio of the response. Figure 1 portrays this comparison.

Fast Sine Sweeps

Several points need to be made if the discussion is limited at this time to fast sine sweeps. On first thought, a linear sweep rate might seem an obvious candidate for use in testing, since its amplitude spectrum is flat. With a flat spectrum, it seems reasonable to just measure the response and use Fourier transform techniques to obtain an estimate of the transfer function. This, of course, is invalid since the phase spectrum of the force has been ignored. In the case of the swept sine, the phase spectrum is a very rapidly rotating vector. When the transfer function calculation is made by either the response transform divided by the force transform or the cross-power spectrum divided by the auto-spectrum of the force, the effect of this rapidly rotating phase vector is accounted for. Of the three fundamentally different sweep rates, linear, log, and exponential, the log seems to represent the best compromise for a lightly damped multiple degree-of-freedom mechanical system with roughly the same damping in each mode. The exponential sweep would impart equal energy into each mode (approximately), but the dynamic range requirements of the analog-to-digital converter to measure the forcing function would be severe when attempting to cover a large swept bandwidth. Likewise, a linear sweep rate would require a large dynamic range to measure the response, since the high frequency modes would reach a much larger percentage of steady-state response.

Better experimental results have been obtained using the periodic log swept sine-forcing function by actually making the function a true transient signal. Since timing is critical in making a truly periodic forcing function in the Fourier analyzer's sample time (T), a transient signal that allows time for the response to die out before the time sample T has been taken is sometimes used. This is accomplished by stopping the sweep typically at 85% of the total time sample taken. The modal damping values of the system under test will dictate this value. Lightly damped systems may require stopping the sweep at 70%. In any event, the sweep is stopped, allowing enough time for the system to decay out to roughly 10% or less of its peak response. To soften startup and shutdown transients, the amplitudes of the sweep time history are also linearly ramped using a 5% ramp time at the beginning and end of the sweep.

Relative to the time domain measurements, the swept sine has an appealing nature over random in that as each resonance is traversed, the response blossoms, giving a quick intuitive feel as to signal-to-noise ratios and system dampings. Data dropouts and other anomalies are much easier to recognize using sine versus random.

Variance Reduction

For measurements made in very noisy environments such as wind tunnel subcritical response tests, the transfer function is composed of a series of swept sine tests (ensembled) averaged together. The coherence function has been used to obtain a measure of the quantity of ensemble averages that should be taken. Wind tunnel testing is considered the worst case for the method, since the ratio of energy input via the sine sweep to the energy input from turbulence is not very high, typically only 2 to 1. To keep the test times under control, usually not more than ten ensembles are used. The resulting transfer functions contain considerable noise or variance on the measurement. This variance problem has now been significantly reduced by the application of an exponential window applied to the raw, measured, system impulse response. The transfer function is obtained and inverse transformed to obtain the system impulse response. Conceptually, this windowing process arises from the characteristics of a systems impulse response, in that it approaches zero with increased time. Because

of the effects of turbulence, the measured impulse response contains extraneous information out beyond the point where, for all practical purposes, the energy within the system has decayed out. These extraneous data produce the major component of the variance observed in the raw transfer function measurement. The multiplication of the raw impulse response by an exponential window suppresses this extraneous information, significantly reducing the variance in the transfer function when the windowed impulse response is inverse transformed. The choice of an exponential window arises from the ease of calculating the correction factor to back out the effects of the window.

Window Correction Derivation

As a starting point, consider a single degree-of-freedom system mapped in the s-plane:

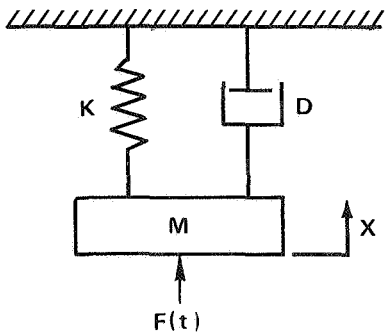

The differential equation of this system is:

$$M\ddot{X} + D\dot{X} + KX = F(t)$$

Using Laplace transform representation with all initial conditions equal to zero:

$$(Ms^2 + Ds + K)\, X(s) = F(s)$$

The transfer function is:

$$H(s) = \frac{X(s)}{F(s)} = \frac{1}{Ms^2 + Ds + K} = \frac{1/M}{s^2 + \frac{D}{M}s + \frac{K}{M}}$$

For convenience, let:

$$A = 1/M,\ B = D/M,\ C = K/M$$

then:

$$H(s) = \frac{A}{s^2 + Bs + C}$$

The roots of this system for the under damped case are:

$$s = -\frac{B}{2} \pm j\sqrt{C - \frac{B^2}{4}}$$

let:

$$\frac{B}{2} = \alpha \qquad \sqrt{C - \frac{B^2}{4}} = \beta$$

then:

$$H(s) = \underbrace{\frac{a}{s + \alpha + j\beta}}_{\text{Negative pole}} + \underbrace{\frac{a^*}{s + \alpha - j\beta}}_{\text{Positive pole}}$$

where:

j	=	the imaginary operator
a	=	a complex constant (residue)
*	=	denotes conjugate

Evaluating the constant a:

$$a = \left.\frac{A}{s + \alpha - j\beta}\right|_{s=-\alpha-j\beta} = \frac{A}{-j2\beta} = j\frac{A}{2\beta}$$

then, in partial fraction form:

$$H(s) = \frac{j\frac{A}{2\beta}}{s + \alpha + j\beta} + \frac{-j\frac{A}{2\beta}}{s + \alpha - j\beta}$$

This system then gives a conjugate pair of poles.

The system parameters are then completely described by three constants; α, β, and the residue (complex constant in the numerator). The natural frequency of the system is:

$$\omega_N = (\alpha^2 + \beta^2)^{1/2} \text{ rad/sec}$$

The damped natural frequency is:

$$\omega_{N_d} = \beta \text{ rad/sec}$$

The damping factor or ratio is:

$$\gamma = \frac{\alpha}{\omega_N}$$

The eigenvector is associated with the residue.

Repeating the Laplace domain description of a single degree-of-freedom system in partial fraction form:

$$H(s) = \frac{j\frac{A}{2\beta}}{s + \alpha + j\beta} + \frac{-j\frac{A}{2\beta}}{s + \alpha - j\beta}$$

where:

A = 1/M

B = D/M

C = K/M

α = B/2

β = $(C - B^2/4)^{1/2}$

M = Mass

D = Damping

K = Stiffness

Taking the inverse Laplace transform of the above equation results in the systems impulse response, $f(t_i)$:

$$f(t_i) = \epsilon^{-\alpha t}\left[\frac{A}{\beta}\sin \beta t\right] \quad t > 0$$

Multiplying the impulse response by the exponential window results in the following:

$$f(t_i) = \epsilon^{-(\alpha+\alpha')t}\left[\frac{A}{\beta}\sin \beta t\right]$$

The only effect the window has on the single degree of freedom is that of increasing the apparent system damping.

In a typical application of this window using the Fourier analyzer:

$$\Delta t = T/N$$

where:

Δt = time between samples in the analog-to-digital sampling, sec

T = total length of time samples, sec

N = total number of samples (channels)

$\epsilon^{-\alpha' t}$ is made equal to 0.1 at channel 1000 (1000 times Δt); therefore:

$$\ell n\,[\epsilon^{-\alpha' t}] = \ell n\,[0.1]$$

$$\alpha' t = 2.30258$$

$$\alpha' = \frac{2.30258}{t_{1000}}$$

where t_{1000} = 1000 times Δt.

The damping ratio of the system without the window is:

$$c/c_0 = \frac{\alpha}{\omega_N}$$

The apparent damping ratio of the system with the window is:

$$c'/c_0 = \frac{\alpha + \alpha'}{\omega_N}$$

since:

$$c/c_0 = \frac{\alpha}{\omega_N}$$

$$\alpha = (c/c_0)\,\omega_N$$

and:

$$c'/c_0 = \left[(c/c_0)\,\omega_N + \alpha'\right]\frac{1}{\omega_N}$$

$$c/c_0 = c'/c_0 - \frac{\alpha'}{\omega_N}$$

$$c/c_0 = c'/c_0 - \frac{(2.30258)}{\Delta t\,(1000)\,(\omega_N)}$$

If the window is applied n times; i.e., the impulse response of the system is multiplied by the window n times,

then:

$$c/c_0 = c'/c_0 - \frac{n\ (2.30258)}{1000\ (\Delta t)\ \omega_N}$$

In the practical application of this windowing technique to reduce the effect of variance due to turbulence, some undesirable effects arise. In a multiple degree-of-freedom system with closely spaced modes (i.e., a pair of roots nearly identical), the application of this window tends to smear the modes together, so that their individual identity tends to merge into what appears to be only one mode. A second practical problem arises because of the truncation of the measured transfer function. In a typical measurement, the transfer function is defined from zero frequency to an upper frequency of interest. When the higher frequency cutoff point coincides with a system antiresonance, no significant problem develops if this antiresonant point has a small magnitude relative to the midband magnitude value. If the upper frequency point coincides with a resonance point, a problem arises due to the truncation of the transfer function. The effect of this truncation is a convolution of the impulse response with a sync function (sin (X)/X). A physical interpretation of this transfer function truncation would be a system impulse response that begins responding before it is excited. This unrealizable impulse response is what would analytically be required to produce the unrealizable truncated transfer function.

In a case where the truncation of the transfer function would produce such an effect, the application of the exponential window would eliminate the tail or convolution product so that when the inverse transform was taken (on the windowed impulse response), the discontinuity in the original transfer function (truncation) would not be reproduced. A modified window is used in such cases to overcome the dominate effects of this problem and allow the tail to be unmodified by the window.

Figure 2 presents a typical transfer function as measured in the wind tunnel on a flutter model. The variance problem makes the measurement a questionable value. This particular measured transfer function also has a truncation problem, since the magnitude is not near zero at the highest frequency in the analysis.

Figure 3 is the calculated impulse response from the raw transfer function measurement of figure 2. The tail at the end is the result of the truncation of the transfer function. Figure 4 presents the exponential window used. The modified window used is dependent upon an observation of the raw impulse response tail. The number of channels (time samples) at which the modified window is at a constant value of unity is arrived at by engineering judgment after observing the raw impulse response. It has been found that there is considerable leeway without any noticeable change in the final windowed transfer function. Figure 5 presents the final transfer function after windowing using the modified window. By whatever method is used to obtain the system frequencies and apparent dampings, the corrected damping could be obtained by using the procedures of this report.

System Identification

With respect to the problem of obtaining a measurement of the complex structural transfer function either in a laboratory environment or a wind tunnel or flight environment, the Fourier analyzer has demonstrated its speed and dynamic range superiority over sine steady-state test methods. The remaining problem, common to both test methods, is that of interpretation of the measured results. Generally, this remaining problem is the methodology used to decompose the measured complex plane transfer function $H(j\omega)$ to separate the total vector response into a set of

linear independent single degree-of-freedom systems so that, when all the individual single degree of freedoms are added together frequency by frequency, the result matches the original measured complex plane measurement. In the past, the methods of Kennedy-Pancu have been used in an attempt to reduce the complex plane plots into a set of modal frequencies and dampings. This method has been reasonably successful when the modes are not too closely spaced. Modes that have become highly damped cannot be tracked by this method either.

The determination of mode shapes from these complex plane plots also becomes invalid for systems having complex eigenvectors. Complex eigenvectors (nonorthogonal vectors) arise when the system damping matrix is not proportional to the stiffness and/or mass matrix. The Laplace transform offers a convenient method whereby both real and complex systems can be analyzed, and it offers a procedure whereby the transfer function measurements can be reduced to modal coordinates of frequency, mode shape, and modal mass, stiffness, and damping.

An airplane in flight exhibits complex modal response due to the aerodynamic forcing terms. Better system identification can thus be realized if the normal assumption of orthogonality is removed.

Laplace Transform

The Fourier transform is basically a two-dimensional representation or picture of a three-dimensional Laplace transform. Consequently, when a transfer function $H(j\omega)$ is obtained and it is desired to identify the system's natural frequencies, dampings, etc., the missing third dimension has to be inferred. The Kennedy-Pancu technique inferrs the third dimension (indirectly), based upon some rather severe assumptions. In many cases, these assumptions are violated, making the technique of limited value. The problem of transfer function interpretation would disappear if a three-dimensional measurement was made. This three-dimensional representation appears via the Laplace transform (fig. 6). The Fourier transform is the plane through $\sigma = 0$ on the $j\omega$ axis of the three-dimensional Laplace (s) domain. If a Laplace transform representation was obtainable from measured data, a complete linear description of the dynamics of the system could be obtained.

A program exists on the Hewlett Packard 5451B Fourier Analyzer (HP) entitled "Modal Analysis System" (refs. 6, 7, 8, and 9), which takes the measured transfer functions (Fourier descriptions) and obtains a Laplace description via a least squares fit. The use of this program has shown encouraging results. For systems which are not too highly damped and for which reasonable measurements of the transfer function have been made, results have been excellent.

Figure 7 contains results of using the modal analysis system on transfer functions measured in flight. The fit was initially performed on the windowed transfer function (fig. 7a) to obtain a better feel as to the quality of the fit (fig. 7b). The results of the fit from the windowed data were used as starting values for the fit on the raw transfer function (fig. 7c). The fit of the raw data is shown in figure 7d. Table 1 presents the comparison of system identification using Kennedy-Pancu's methods on the windowed data, the HP modal analysis on the windowed data, and the HP modal analysis on the raw data. This particular data set was obtained using only one sweep ensemble. The results compare favorably.

An intriguing aspect of obtaining a Laplace description of an airplane transfer function in flight is that, if it were possible, this result coupled with the measured zero airspeed Laplace description could result in a measured Laplace description for the aerodynamic forcing function.

The Laplace approach is still left with some assumptions; i.e., we still can only handle linear systems, and the system under test cannot as yet have multiple roots—more than one mode with the same frequency *and* damping. The modal analysis system has handled systems with identical damped natural frequencies (same value for $j\omega$), if the damping values are considerably different.

EXPERIMENTAL STUDIES

Early Tests

In the first applications of the Fast Fourier Transform (FFT) techniques, existing off-line data processing with existing computing facilities was employed. In these early trials, existing or modified computer programs were used to compare the analytically and experimentally determined transfer functions of simple analogue systems. This work was then expanded to use available dynamic models where the practical problems of nonlinear structural effects and uncorrelated forcing functions (atmospheric turbulence) could be studied.

The first application of the FFT techniques on a Boeing aircraft came in a ride improvement program for the 747 (ref. 10). The objective of this testing was to develop an active control system to improve the ride qualities of the aircraft by suppressing the response of the aircraft's flexible modes of vibration. To aid in this work, the FFT techniques were used to derive the transfer functions between the motions of various locations in the aircraft and forcing functions applied through the aircraft's yaw damper servo units. Both pseudorandom and sinusoidal fast sweep excitation signals were initially employed in this testing; but, because of the greater energy input from the sinusoidal sweep excitation, this form of excitation rapidly became the only one used in later tests.

A typical plot generated from the testing is shown in figure 8. Despite testing in turbulent air and the lack of experience in variance reduction techniques, the tests generated sufficient data to enable the definition of the required transfer functions and the successful development of an active control system.

The results of this testing were also sufficiently encouraging for the technique to be used as a primary analysis system in the AWACS Brassboard ground vibration test where, by a microwave link to a remote computer, data reduction was achieved in a near real-time manner by personnel at the test site. However, since at this time the analysis systems were only capable of generating transfer function plots, considerable manual data reduction was necessary to generate modal frequencies, damping, and mode shapes of the structure from such plots.

Following this work and as a part of the SST Follow-On program conducted by The Boeing Company, a low-speed flutter model was used to demonstrate transient testing techniques that might be developed for wind tunnel and flight flutter testing of future aircraft. This work (ref. 11) considered the use of both fast sinusoidal sweep and pseudorandom noise excitation in comparison with steady-state excitation.

As previously discussed, the fast sinusoidal sweep excitation enables more energy to be input to a system within the same maximum excitation level. The results of this testing demonstrated in a practical manner the superiority of the fast sinusoidal form of excitation and also marked the first use of Hewlett Packard's Fourier analyzer for on-line data reduction.

More recently a series of data recorded during testing as the tunnel airspeed was increased toward the flutter speed has been reanalyzed using the current system capabilities of windowing the

data (fig. 9). A comparison of these results with those presented in reference 11 allows more modes to be identified from the data, providing a greater understanding of the system.

YC-14 Low-Speed Flutter Model

Vibration testing of a low-speed flutter model, both in still air and during wind tunnel testing using the current system capabilities, has been conducted as part of a test program to verify analytical flutter predictions for the aircraft. The use of the system during still air testing enabled a rapid identification of the natural frequencies and damping of the vibration modes, while mode shapes were generated from measurement of the responses at a large number of points across the model. A comparison of the test and analysis frequencies is given in table 2.

In the wind tunnel testing of a cantilevered empennage model (fig. 10), a floor-mounted electrodynamic exciter was used to provide the necessary excitation force, while accelerometers within the model recorded the model's response. On-line production of the model's transfer functions were then generated as test speeds were increased up to the flutter speed. Figure 11 shows the progressive change in such a set of transfer functions as the tunnel speed was increased. From these transfer functions, modal frequencies and damping were manually reduced, and their variations with airspeed were obtained (fig. 12). The use of this approach enabled a large amount of data to be gathered within a realistic time period for a large number of model configurations. One configuration involving a free mass balanced elevator was tested to high speeds before subcritical testing was conducted at low tunnel speeds to reduce some data scatter. The excitation system here provided the energy to initiate flutter, since tunnel turbulence was very small at these speeds. Figure 13 shows the results for this configuration.

727 Transonic Empennage Flutter Model

The fast sine sweep excitation and FFT data analysis techniques have recently been employed in ground vibration and wind tunnel testing of a 727 transonic flutter model. This test program was conducted to experimentally determine the complete dynamic characteristics of this model for use in theoretical flutter calculations.

During ground vibration testing of the model, the modal frequencies, damping, and mode shapes were reduced on-line using the full capabilities of a Hewlett Packard Dynamic Analyzer (HP-5451B). This system employed the previously discussed Laplace mathematical model fitted to the experimental transfer functions to enable a system's dynamic properties to be extracted.

Mode shapes of all model modes below 75 Hz were determined by making a series of measurements over the model and allowing the analyzer to reduce and plot the natural model modes (fig. 14).

To determine the generalized masses of these modes, the technique of using added incremental masses to the model and observing the change in modal frequency and mode shape was used. This technique is summarized in appendix A. The technique assumes that the model's modes are not complex; i.e., monophase.

Accurate evaluation of modal generalized masses is dependent on accurate determination of the mode shapes. Triaxial mode shapes were carefully measured at the incremental mass location and at a reference location on the model for each mode. Total vector mode shapes were evaluated from the triaxial measurements and were used in the generalized mass evaluation.

The incremental masses were varied in magnitude and location to allow two or three separate determinations of generalized mass for each mode. A comparison of resulting values of generalized mass for individual modes showed an average variation in experimental results of 5%. Table 3 presents the measured modal frequencies and generalized masses.

The experimental values of generalized mass and modal frequencies were used in conjunction with calculated oscillatory aerodynamic coefficients to complete a flutter analysis to predict model behavior. The oscillatory coefficients were calculated using the measured modal displacements as input to Doublet-Lattice Oscillatory Aerodynamics theory.

During wind tunnel testing of the model (fig. 15), sine sweep excitation from 2.5 to 50 Hz of the model was accomplished using an electrohydraulic-actuated aerodynamic vane located at the fin tip leading edge. Model response was monitored and recorded for 12 separate accelerometers located on the model structure.

Each sinusoidal sweep from 2.5 to 50 Hz required approximately 20 sec, and an ensemble of 10 sweeps was completed at each wind tunnel Mach number and pressure condition. The resulting input-to-output response transfer functions were ensemble averaged and windowed to reduce variance in data due to model response from sources other than the sinusoidal aerodynamic vane force. Table 4 compares data reduced by using both the Kennedy-Pancu and the modal data analysis techniques.

Complex vector amplitude plots (fig. 16) were produced in a near-to-real time manner and were evaluated using the methods of Kennedy-Pancu (ref. 1) to provide model response frequency and damping. This data reduction was readily accomplished between wind tunnel conditions and plots of damping; frequency versus wind tunnel dynamic pressure were recorded. The damping magnitude and trends as displayed by continuous (between tunnel condition) plotting were reviewed prior to changing wind tunnel conditions.

Figure 17 presents the damping and frequency trends measured during the 727-300 T-tail flutter model test. The last recorded entry was at 34.5 kPa (720 lb/ft^2) dynamic pressure. While on condition and recording data at 38.3 kPa (800 lb/ft^2) dynamic pressure, a fatigue failure in the fin root structure occurred, and the empennage was separated from the model.

Posttest analyses of the data recorded at this final test condition of 38.3 kPa (800 lb/ft^2) have been conducted using the data analysis system with individual sweep records. Figure 18 shows the variation in the T-tail mode frequency experienced as the fatigue failure progressed. During this time, the transient excitation analysis techniques proved invaluable. A complete understanding of the events resulting in the model destruction would not have been realized if the transient excitation and data processing technique had not beem employed.

747 Derivative Tests

Recently, several derivatives of the Boeing 747 aircraft have been tested using current transient testing techniques. These techniques were used to gather data during the ground vibration tests on the 747SP aircraft, where the closely spaced modes of the aircraft were separated by posttest analysis. Posttest data analysis minimized the impact on the manufacturing production flow of the aircraft.

Flight flutter testing of 747 derivative aircraft has also been conducted using the yaw damper servo on the rudder actuator as a means of excitation at low frequencies. Once again, good results have been obtained in an on-line data reduction mode of operation (fig. 19).

CONCLUSION

The steady development of transient testing techniques employing fast sinusoidal sweep excitation forces in conjunction with Fourier and Laplace transform techniques has generated a powerful test capability for use in the many forms of system identification of which flight flutter testing is a small part.

The experience gained with these techniques has shown them capable of providing a wealth of data to the dynamics engineer. These techniques have also increased the safety of flight testing while also enabling test times to be reduced.

While the analysis system meets present requirements, development continues to increase its capabilities in the bulk of data that can be processed and also in determining the generalized air forces that act on an aircraft in flight.

APPENDIX A

EXPERIMENTAL EVALUATION OF GENERALIZED MASS USING THE INCREMENTAL MASS MEASUREMENT TECHNIQUE

Reference: AGARD, Part IV, section 8.1, pp 24 through 27.

$$S = I\omega^2$$

where:

S = generalized modal stiffness

I = generalized modal mass

ω = modal frequency

With the addition of a small incremental mass (δm) to the structure at a point p:

$$S = (I + \Delta I)\omega_1{}^2$$

where:

ΔI = generalized modal mass increment

ω_1 = modal frequency with incremental mass added

Since the structural stiffness is unaffected by the addition of an incremental mass:

$$I\omega^2 = (I + \Delta I)\omega_1{}^2$$

or

$$\llcorner\phi\lrcorner [J] \{\phi\} \omega^2 = \left[\llcorner\phi\lrcorner [J] \{\phi\} + \phi_p{}^2 \delta m\right]\omega_1{}^2$$

where:

$\{\phi\}$ = modal displacement matrix

ϕ_p = modal displacement vectors at point p

$[J]$ = mass matrix

Rearranging the above equation gives:

$$\llcorner\phi\lrcorner [J] \{\phi\} = I = \frac{\phi_p{}^2 \delta m \omega_1{}^2}{\omega^2 - \omega_1{}^2}$$

showing that the generalized modal mass (I) is a function of the incremental mass (δm); the modal displacement (ϕ_p) at the location δm is attached; and the modal frequencies are evaluated with and without δm in place (ω_1 and ω).

REFERENCES

1. Kennedy, C. C. and Pancu, C. D. P.: Use of Vectors in Vibration Measurement and Analysis. Journal of the Aeronautical Sciences, November 1947.

2. Small, E. F.: Evaluation of Vibration Methods to Separate Closely Spaced Modes. The Boeing Company, D6-9447, TN, May 1968.

3. Olsen, N. L.: Flight Flutter Measurements Using The Analog Aeroelastic Modal Analysis System (AMAS). The Boeing Company, D6-33241, INF., February 1972.

4. Winter, W. A.: Flutter Testing of Aircraft in Flight. British Communications and Electronics, April 1963.

5. White, R. G.: Dynamic Analysis of Structures by Transient Excitation. Thesis, Institute of Sound and Vibration, University of Southampton, March 1970.

6. Olsen, N. L.: Vibration Testing Methods and Techniques–Technical Notes. The Boeing Company, D6-6597, INF., June 1975.

7. Hewlett Packard 5451B Fourier Analyzer System Manuals.

8. Richardson, M. and Potter, R.: Identification of Modal Properties of an Elastic Structure From Measured Transfer Junction Data. 20th International Instrumentation Symposium, Albuquerque, N.M., May 1974.

9. Potter, R. and Richardson, M.: Mass, Stiffness, and Damping Matrices From Measured Modal Parameters. International Instrumentation–Automation Conference, New York, October 1974.

10. Cohen, G. C., Cotter, C., and Taylor, D. L.: Use of Active Central Technology to Improve Ride Qualities of Large Transport Aircraft. NASA Symposium on Active Control Technology, July 1974.

11. Ryneveld, A. D.: Transient Excitation Techniques for Wind Tunnel and Flight Flutter Testing of SST Configurations. SST Technology Follow-On Program–Phase II, FAA-SS-73-14, May 1974.

Table 1.– Comparison of system parameters derived from figure 7.

KENNEDY-PANCU[a]			MODAL ON WINDOWED DATA[a]		
MODE	FREQUENCY, Hz	DAMPING, c/c_0	MODE	FREQUENCY, Hz	DAMPING, c/c_0
1	1.76	0.048	1	1.772	0.0427
2	2.27	0.030	2	2.224	0.0386
3	2.44	0.049	3	2.432	0.0544

MODAL ON RAW DATA

MODE	FREQUENCY, Hz	DAMPING, c/c_0
1	1.768	0.0420
2	2.217	0.0342
3	2.44	0.0528

[a]CORRECTED FOR THE WINDOW.

Table 2.– YC-14 low-speed flutter model comparison of test and analysis results.

MODE	EXPERIMENTAL RESULTS		ANALYTICAL RESULTS, Hz	DESCRIPTION
	FREQUENCY, Hz	DAMPING, c/c_0		
SYMMETRIC MODES				
1	5.68	0.005	5.44	FUNDAMENTAL WING BENDING
2	8.62	0.007	8.47	FUNDAMENTAL WING TORSION
3	10.70	0.002	10.61	NACELLE PITCH
4	13.09	0.001	12.84	WING CHORDWISE, NACELLE SIDE BENDING
5	15.15	0.017	15.07	STABILIZER BENDING
6	15.82	0.003	15.62	
7	16.33	0.006	15.77	
ANTISYMMETRIC MODES				
1	5.41	0.002	5.48	AFT BODY TORSION, STABILIZER ROLL
2	6.93	0.005	6.75	FIN TORSION
3	7.72	0.001	7.69	WING BENDING/TORSION
4	10.49	0.003	10.42	WING BENDING, NACELLE PITCH STABILIZER ROLL
5	11.80		11.85	SECOND WING BENDING STABILIZER ROLL
6	15.42		15.16	NACELLE SIDE BENDING
7	17.45	0.002	17.43	OUTERWING TORSION, WING CHORDWISE STABILIZER BENDING

Table 3.– 727 T-tail model ground vibration test.

MODE	FREQUENCY, Hz	GENERALIZED MASS. kg cm^2 (LB-IN-SEC^2)
1	3.68	388.66 (4.13)
2	8.79	7.067 (0.0751)
3	16.57	1.120 (0.0119)
4	25.40	0.285 (0.00303)
5	34.28	1.223 (0.0130)
6	40.13	5.092 (0.0541)
7	53.21	0.863 (0.00917)
8	65.21	0.882 (0.00937)

Table 4.– Comparison of modal parameters for 727-300 empennage model data (fig. 16).

KENNEDY–PANCU[a]

MODE	FREQUENCY, Hz	DAMPING, c/c_0
1	3.8	0.0162
2	9.3	0.0397
3	16.7	0.0335

MODAL ON RAW DATA

MODE	FREQUENCY, Hz	DAMPING, c/c_0
1	3.77	0.016
2	9.22	0.0371
3	16.765	0.0312

[a]CORRECTED FOR THE WINDOW.

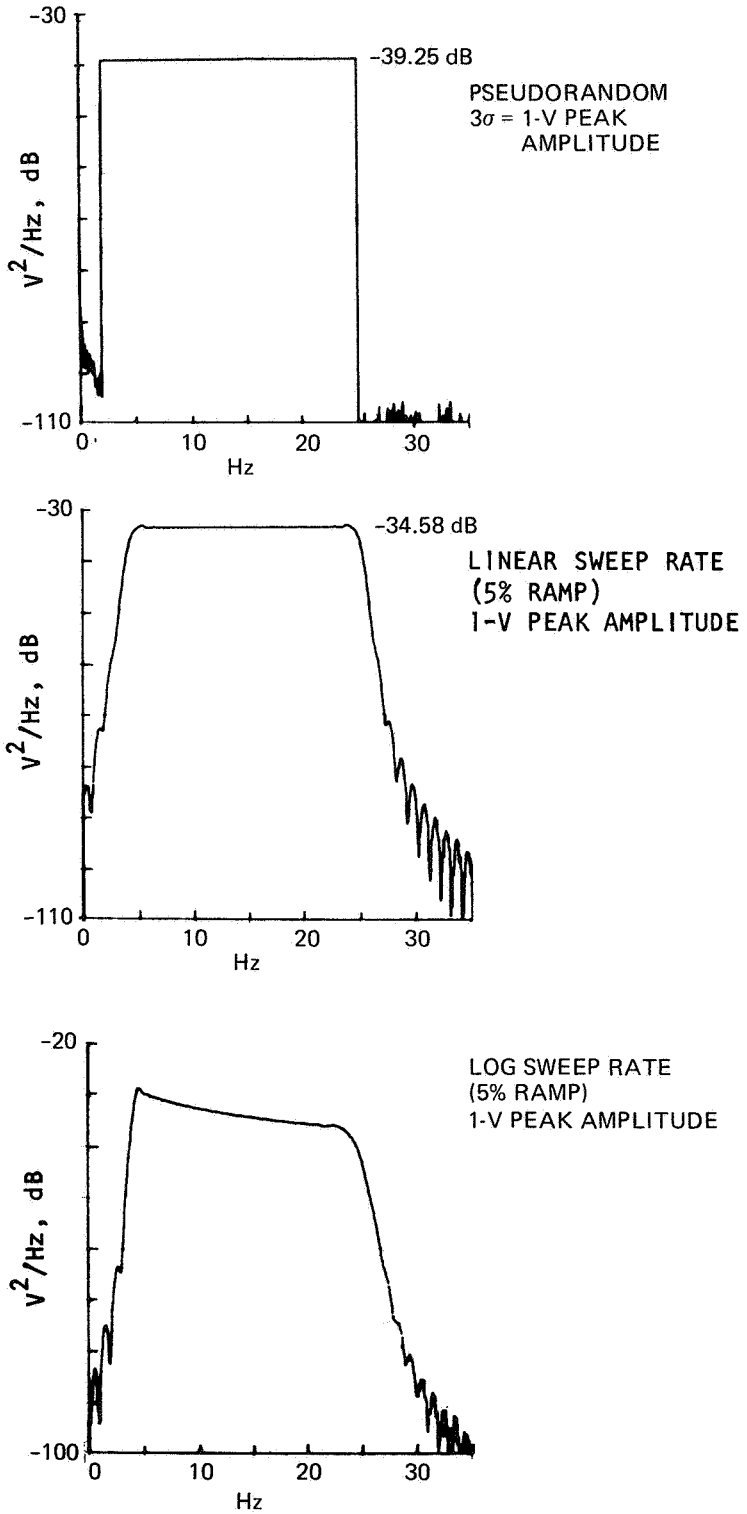

Figure 1.–Comparison of excitation signal input powers, dB.

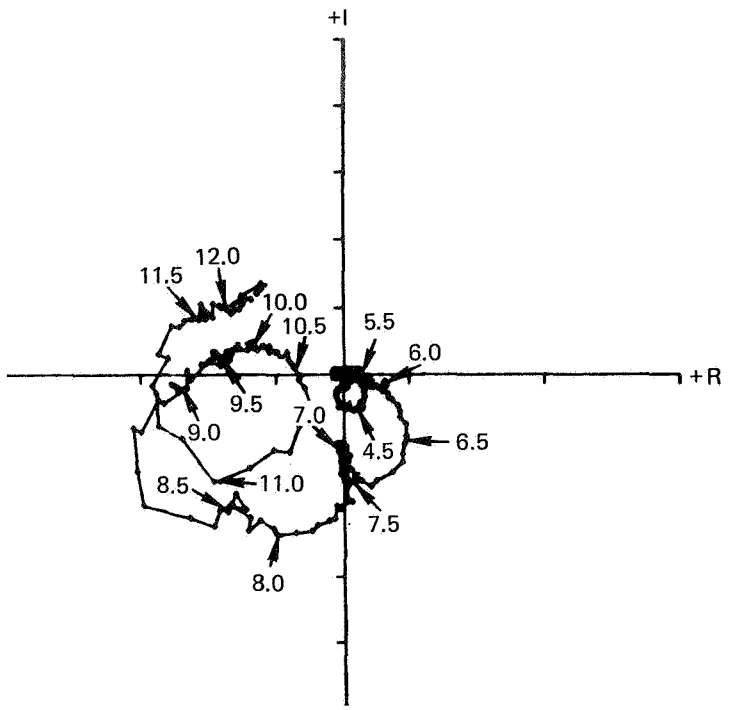

Figure 2.– Raw transfer function from a wind tunnel test.

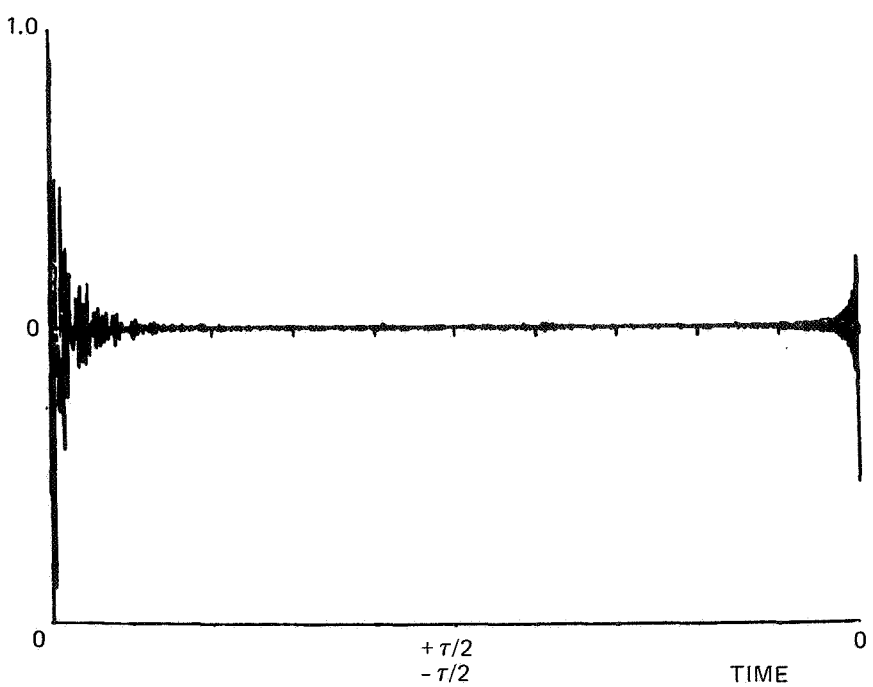

Figure 3.– Impulse response of figure 2.

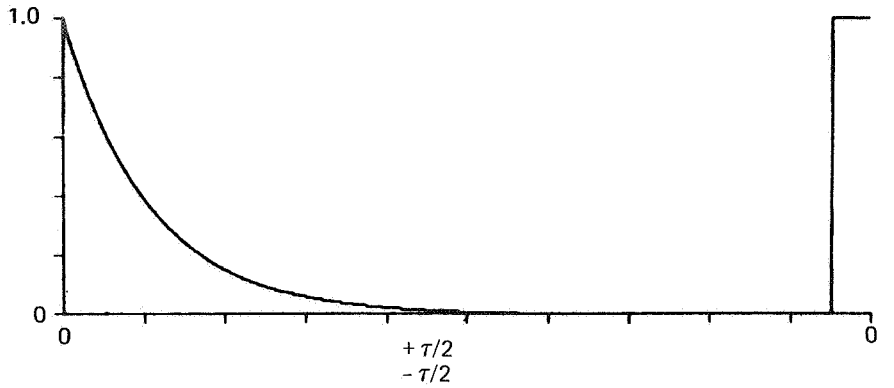

Figure 4.– Typical window function.

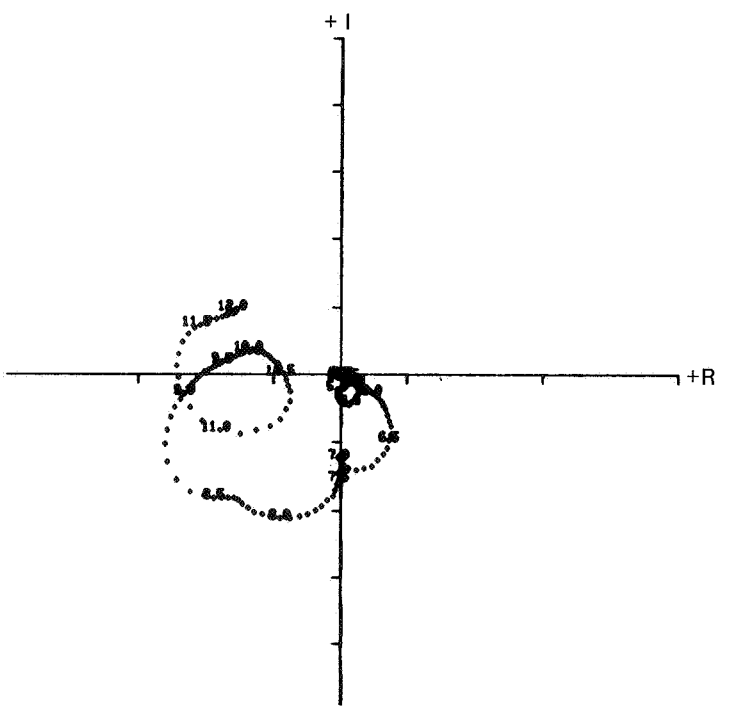

Figure 5.– Windowed transfer function.

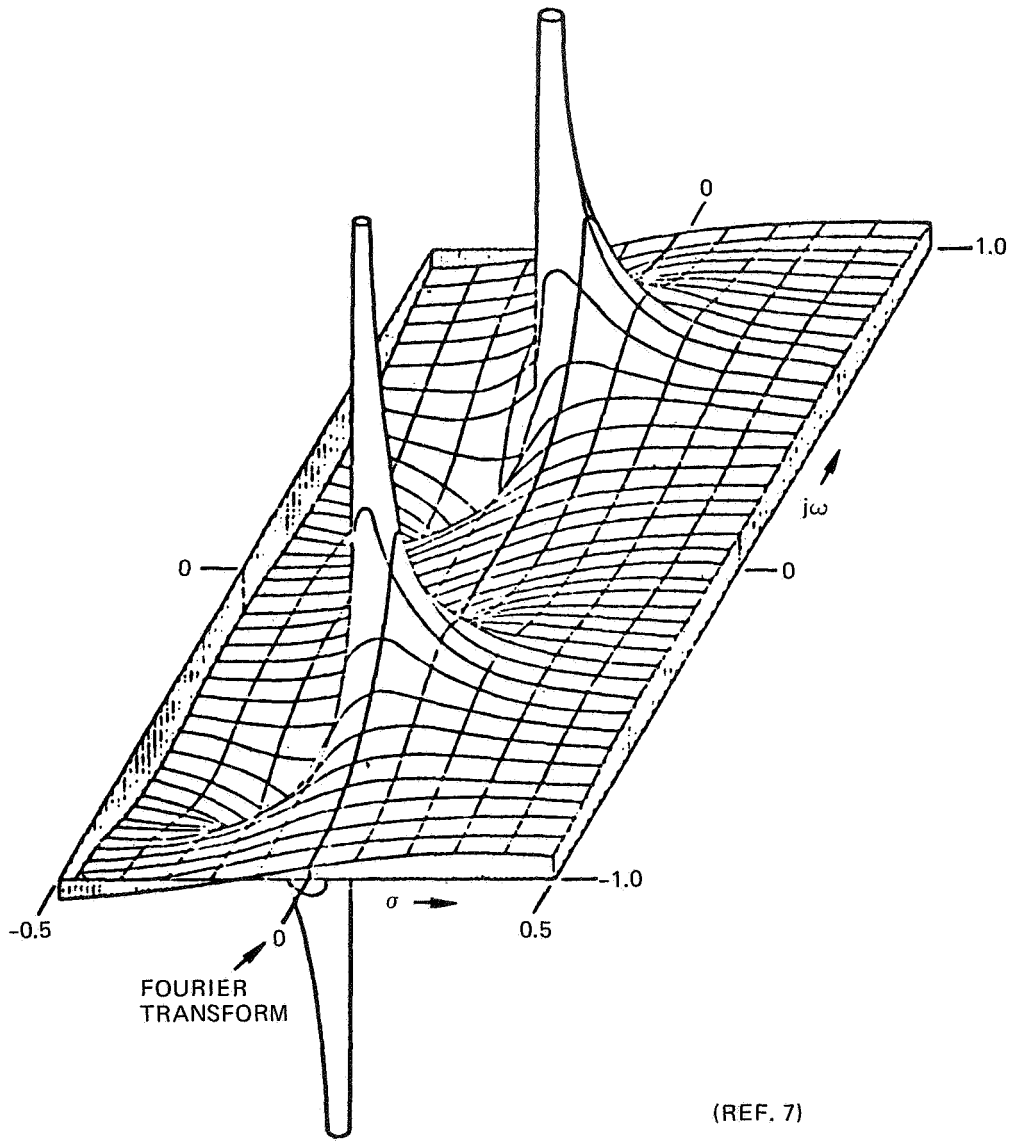

Figure 6.– The imaginary part of the transfer function of a simple resonator with poles at s = -0.1 ±j0.5.

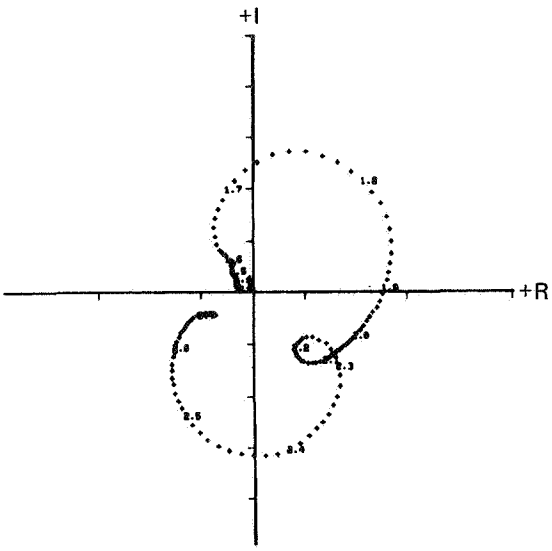

a. Windowed Data

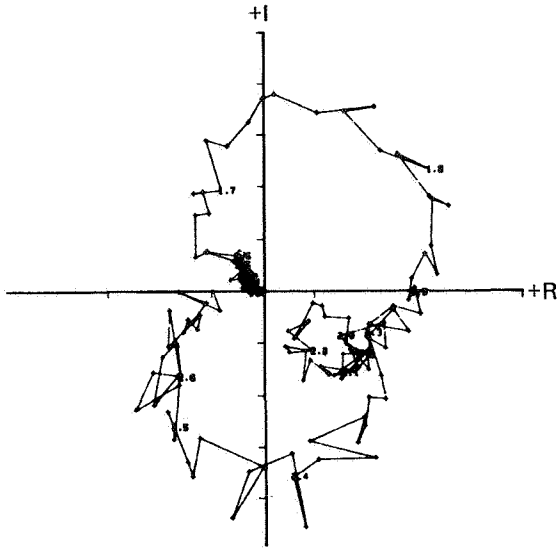

c. Raw Data

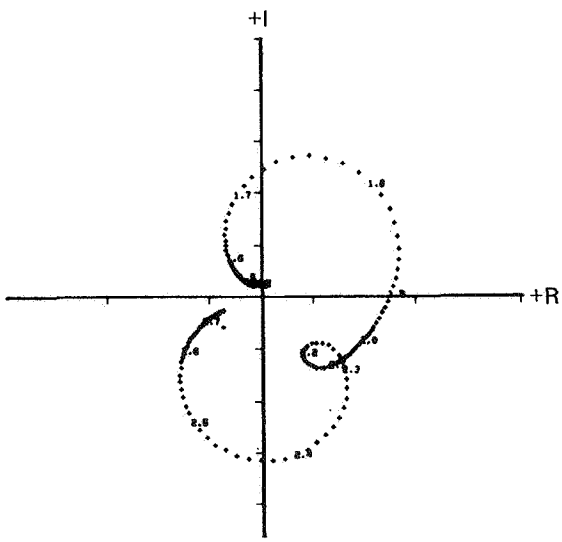

b. Fit of Windowed Data

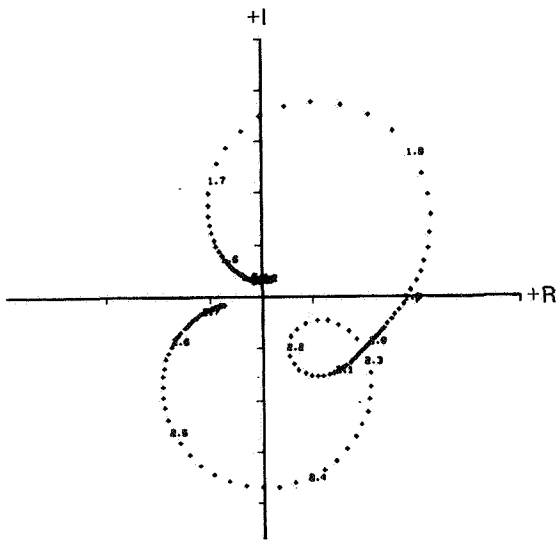

d. Fit of Raw Data

Figure 7.– 747 Flight flutter test–R.H. wingtip/rudder position.

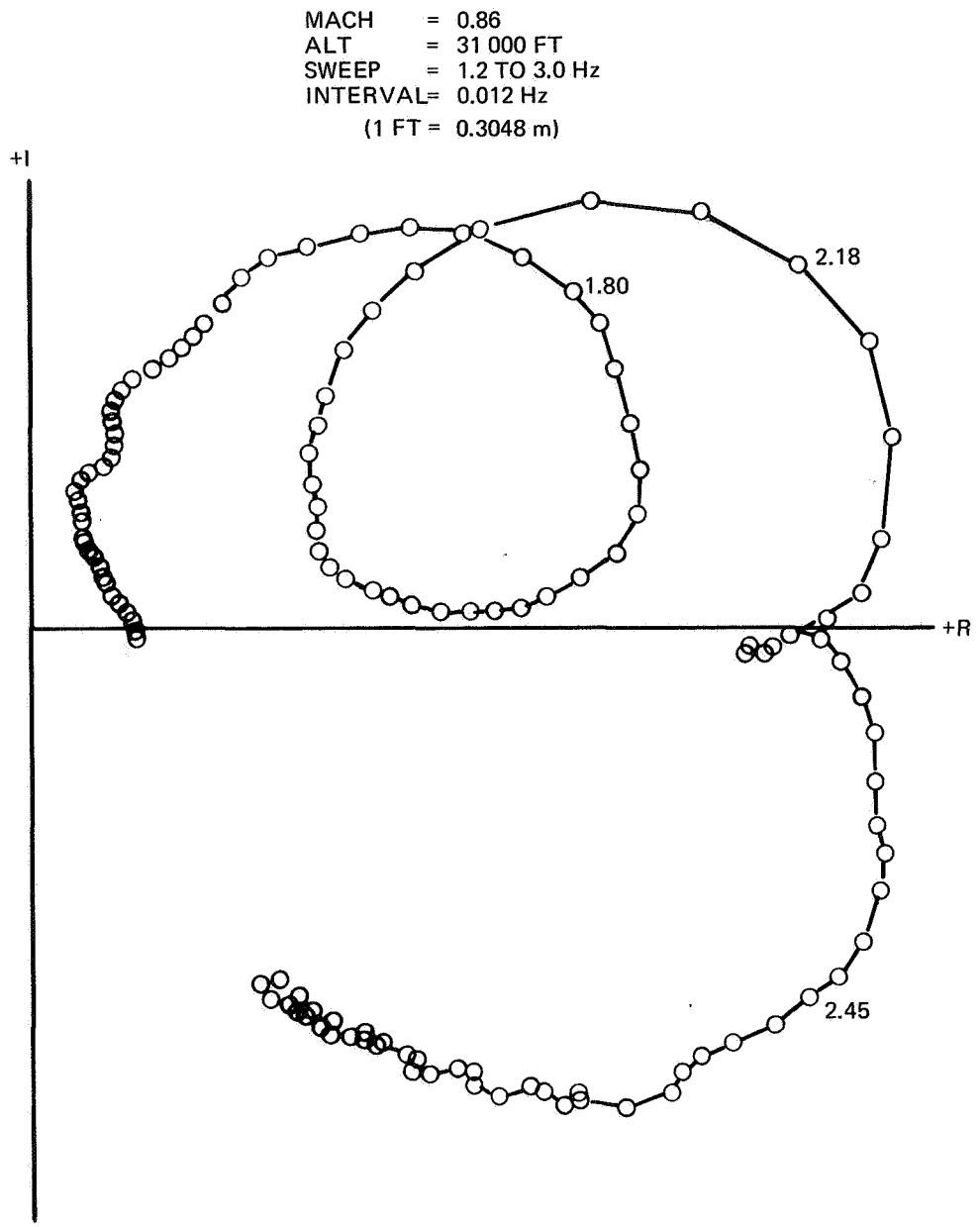

Figure 8.– 747 flight test–Lateral fuselage response to lower rudder yaw damper actuator command signal.

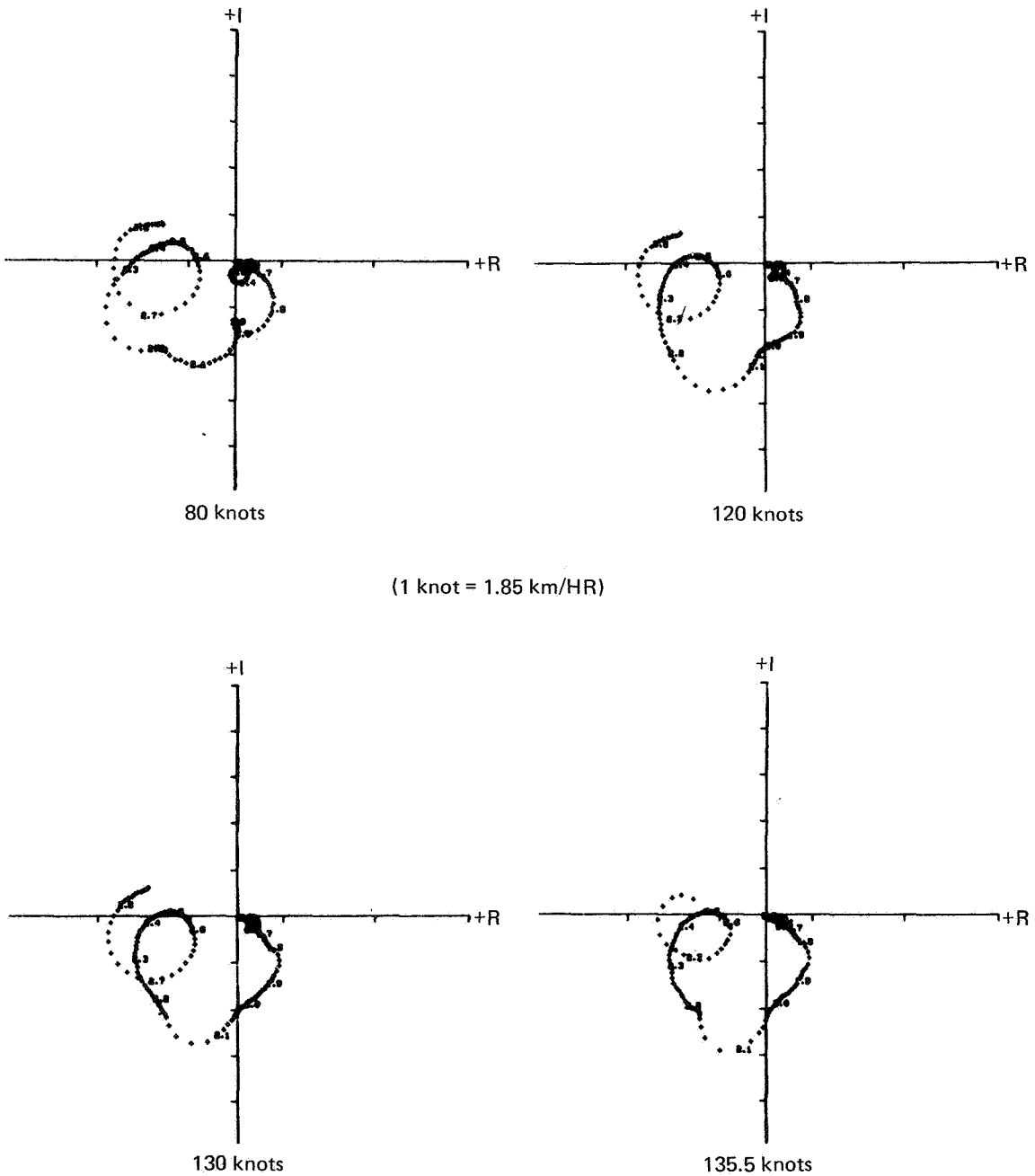

Figure 9.– Transfer functions for windowed data of SST low-speed flutter model (ref 11).

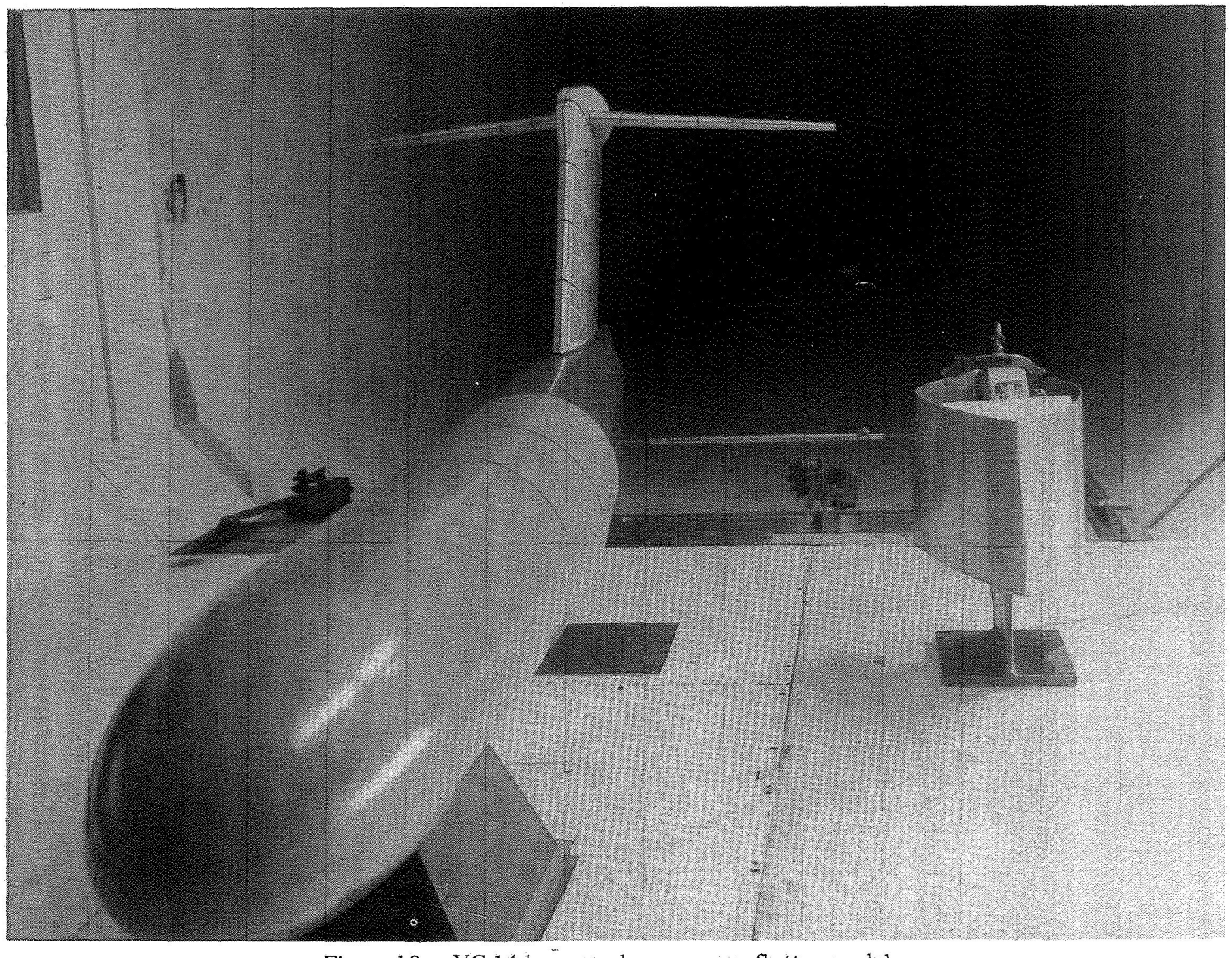

Figure 10.– YC-14 low-speed empennage flutter model.

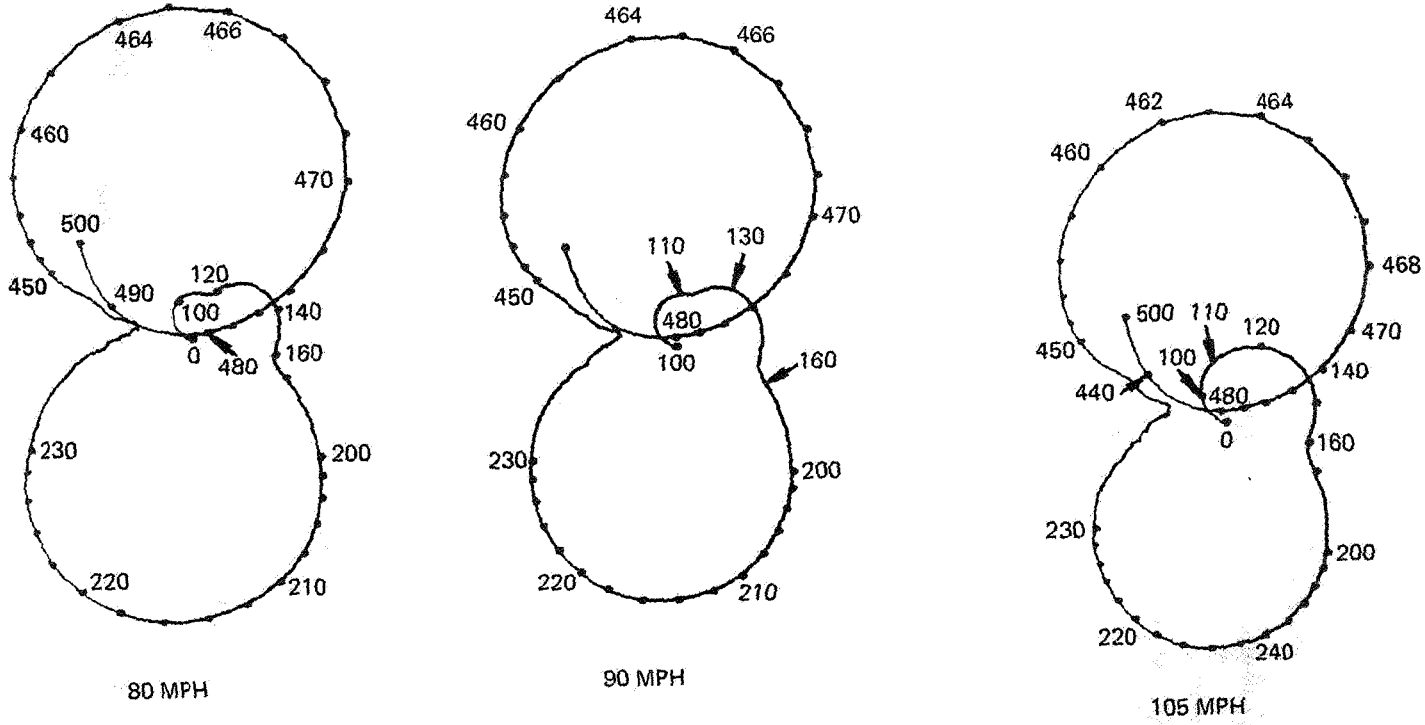

NOTE: FREQUENCY = SCALE NUMBERS X 0.05
(1 MPH = 1.61 km/HR)

Figure 11.– Transfer functions for low-speed YC-14 flutter model at increasing speeds.

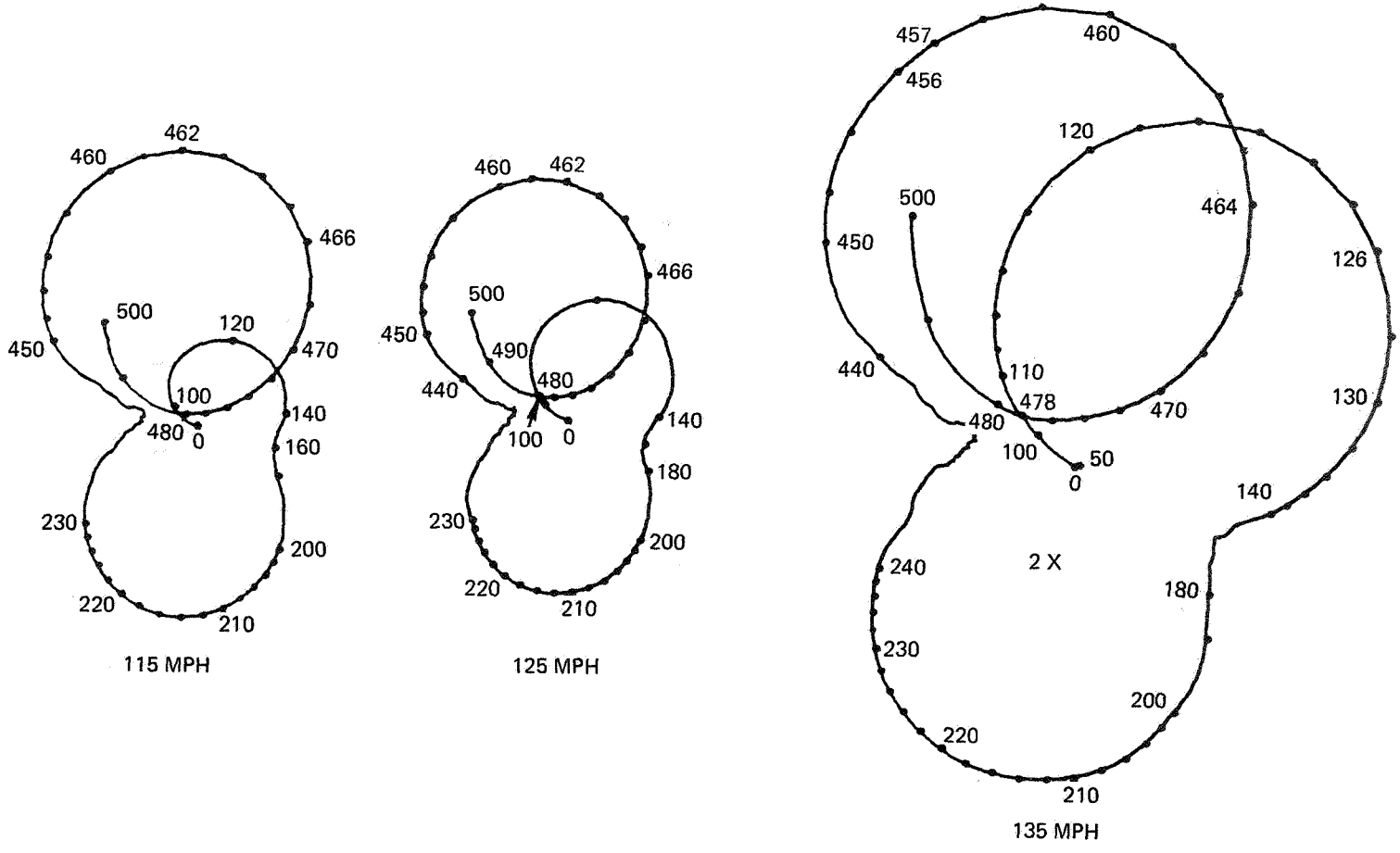

Figure 11.– (Concluded).

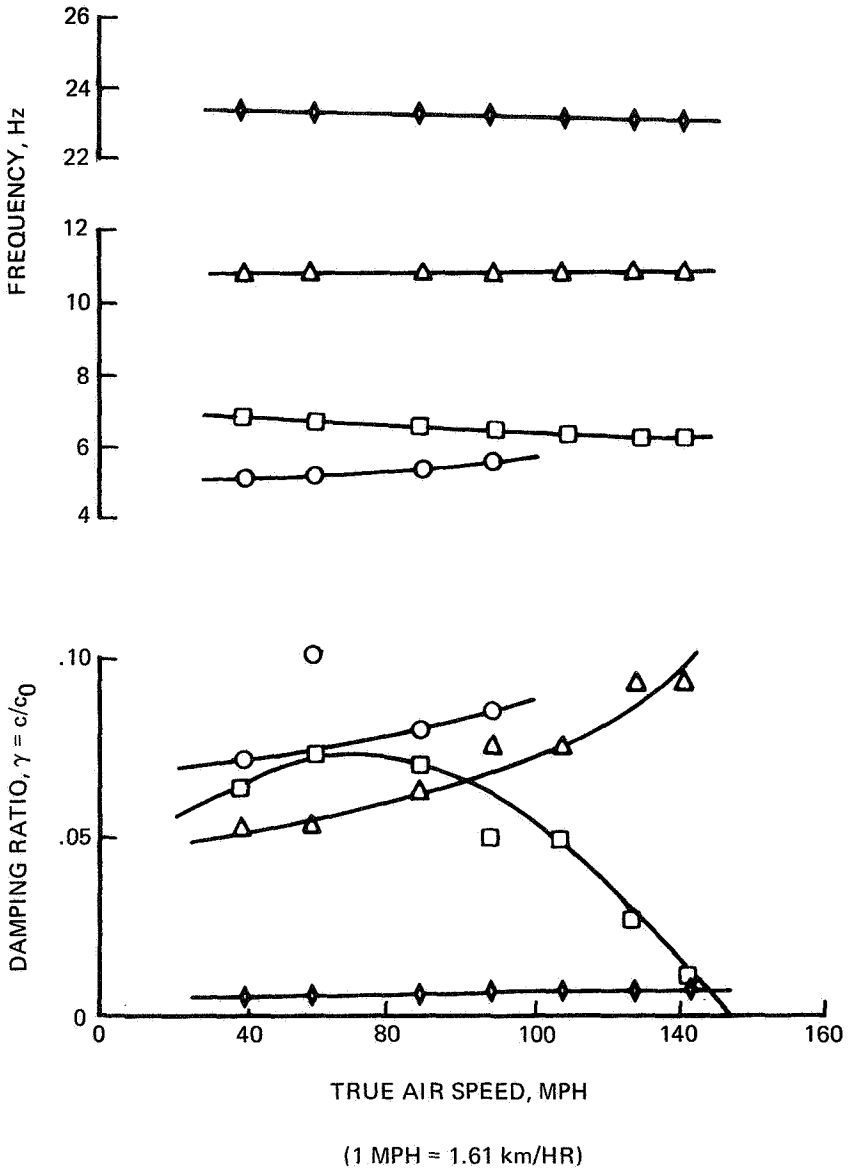

Figure 12.– Variations in modal frequencies and damping derived from figure 11.

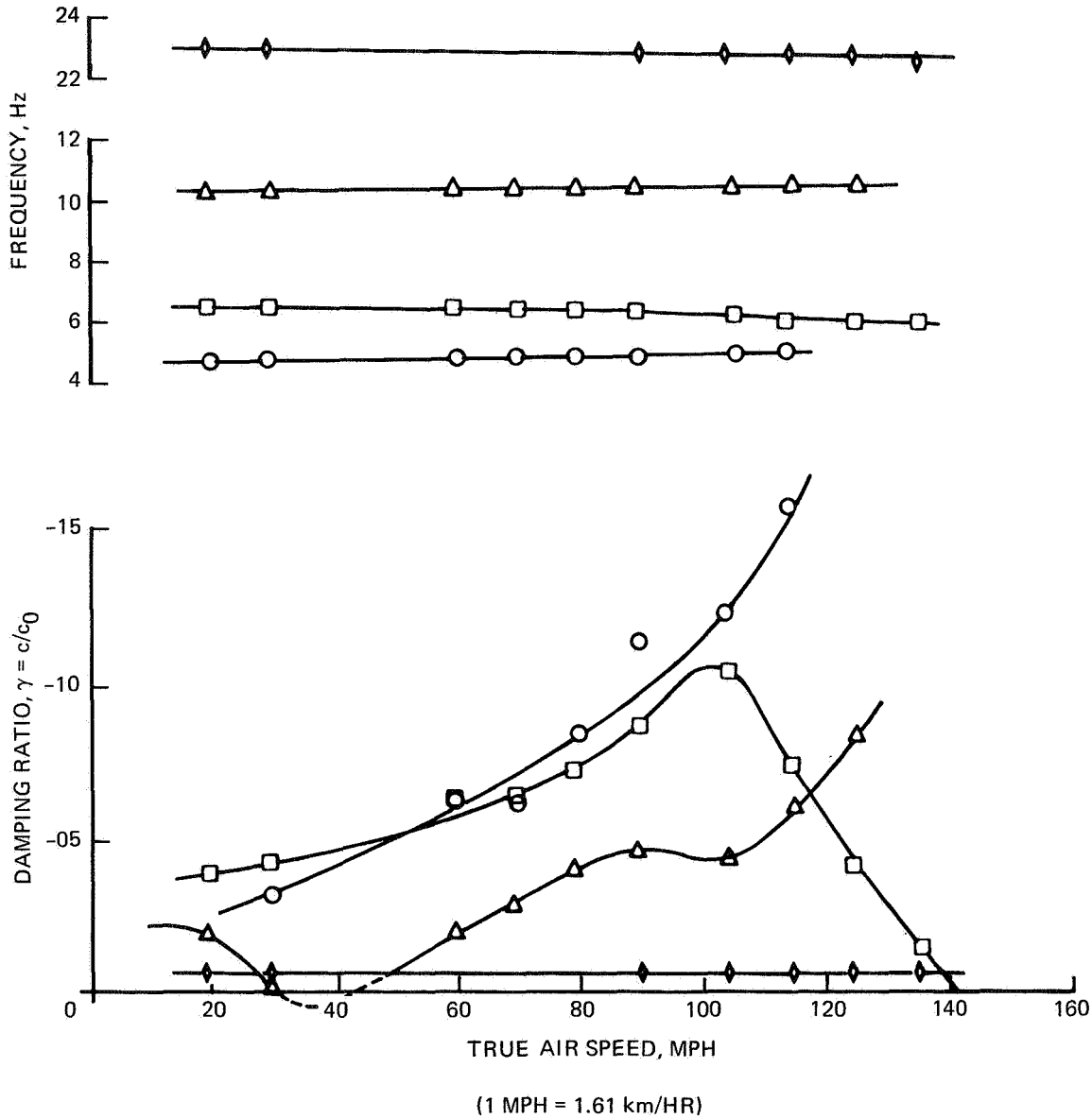

Figure 13.– Frequency and damping variations for model with free elevators.

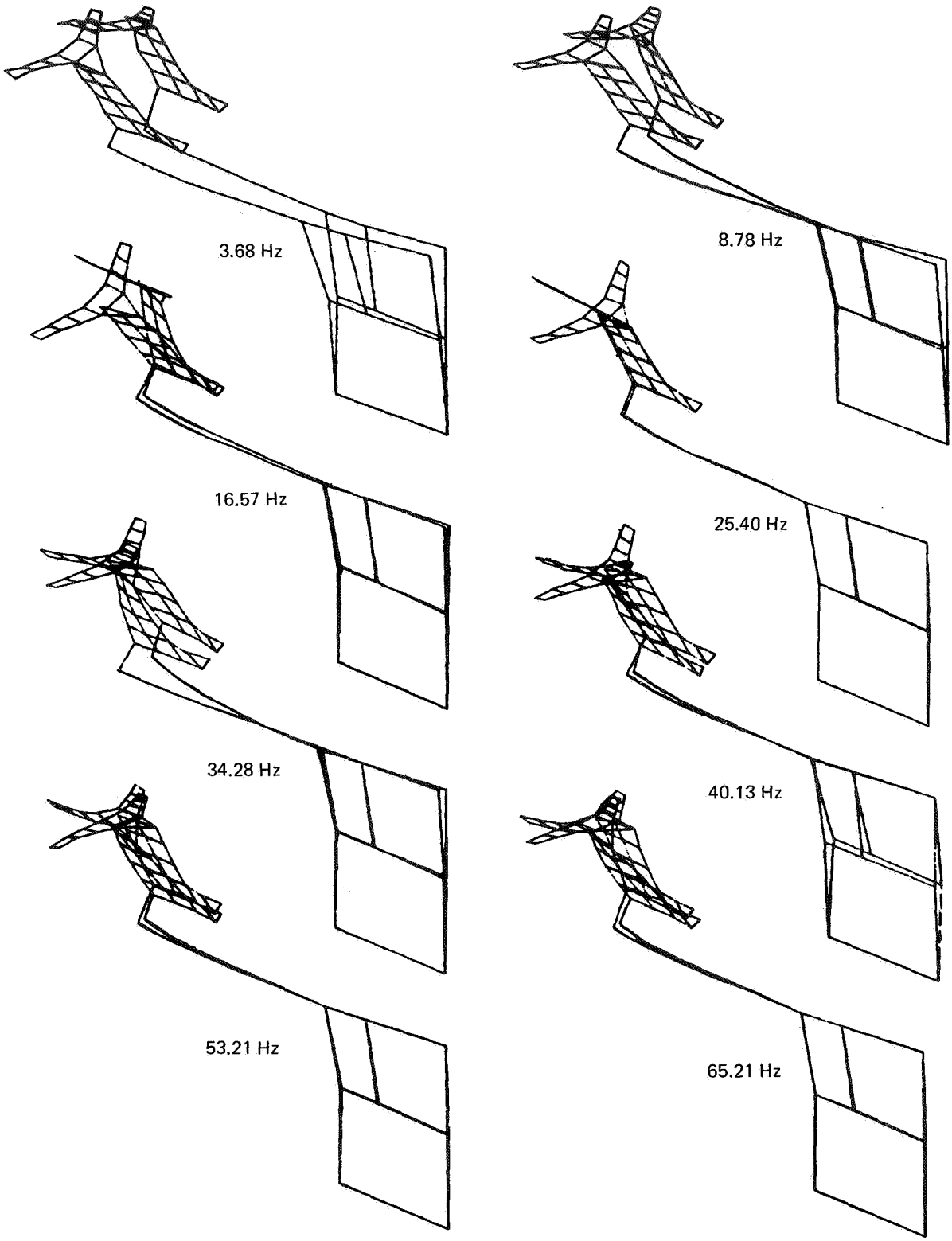

Figure 14.– Still air antisymmetric mode shapes of 727-300 transonic empennage model.

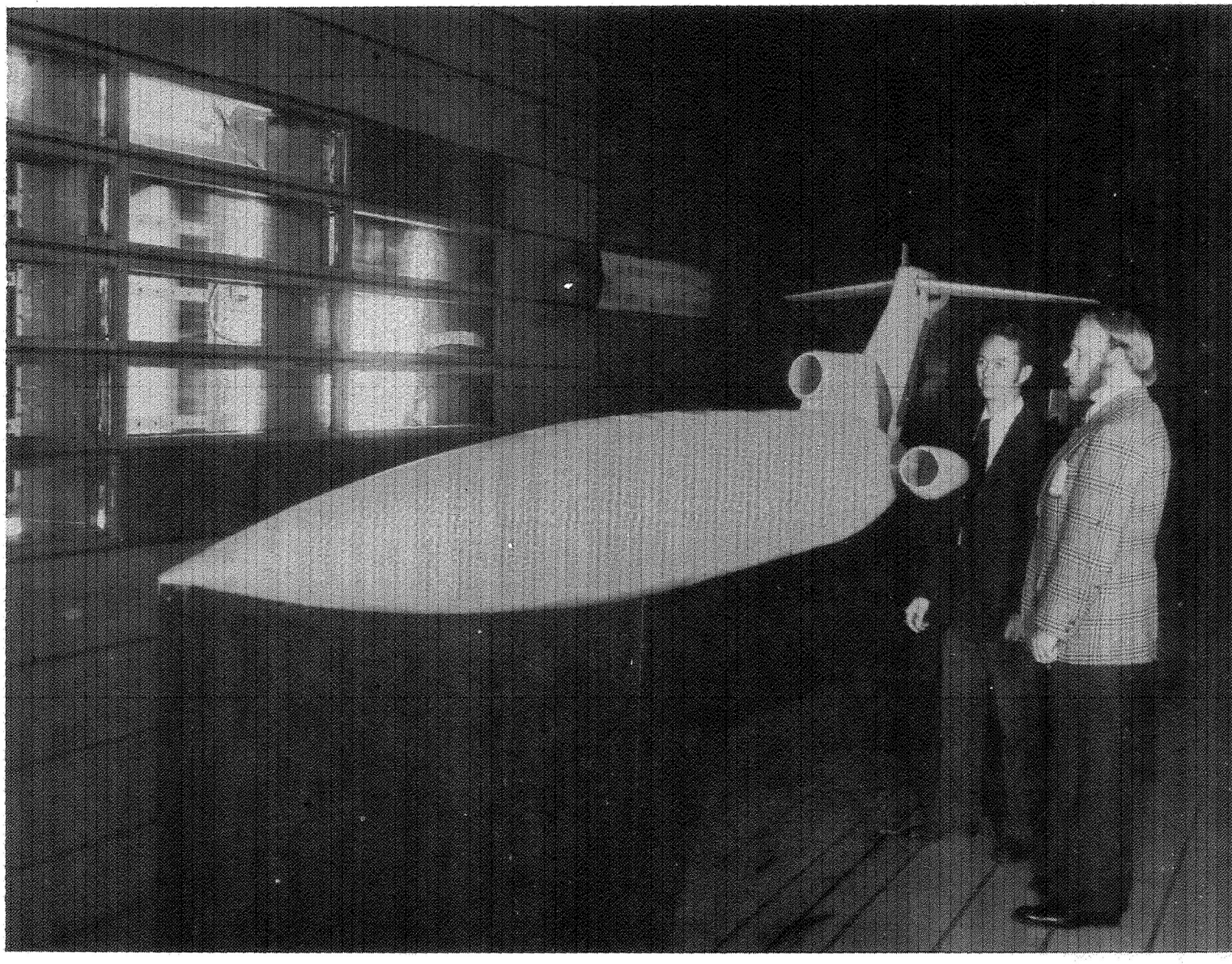

Figure 15.– 727-300 transonic empennage flutter model.

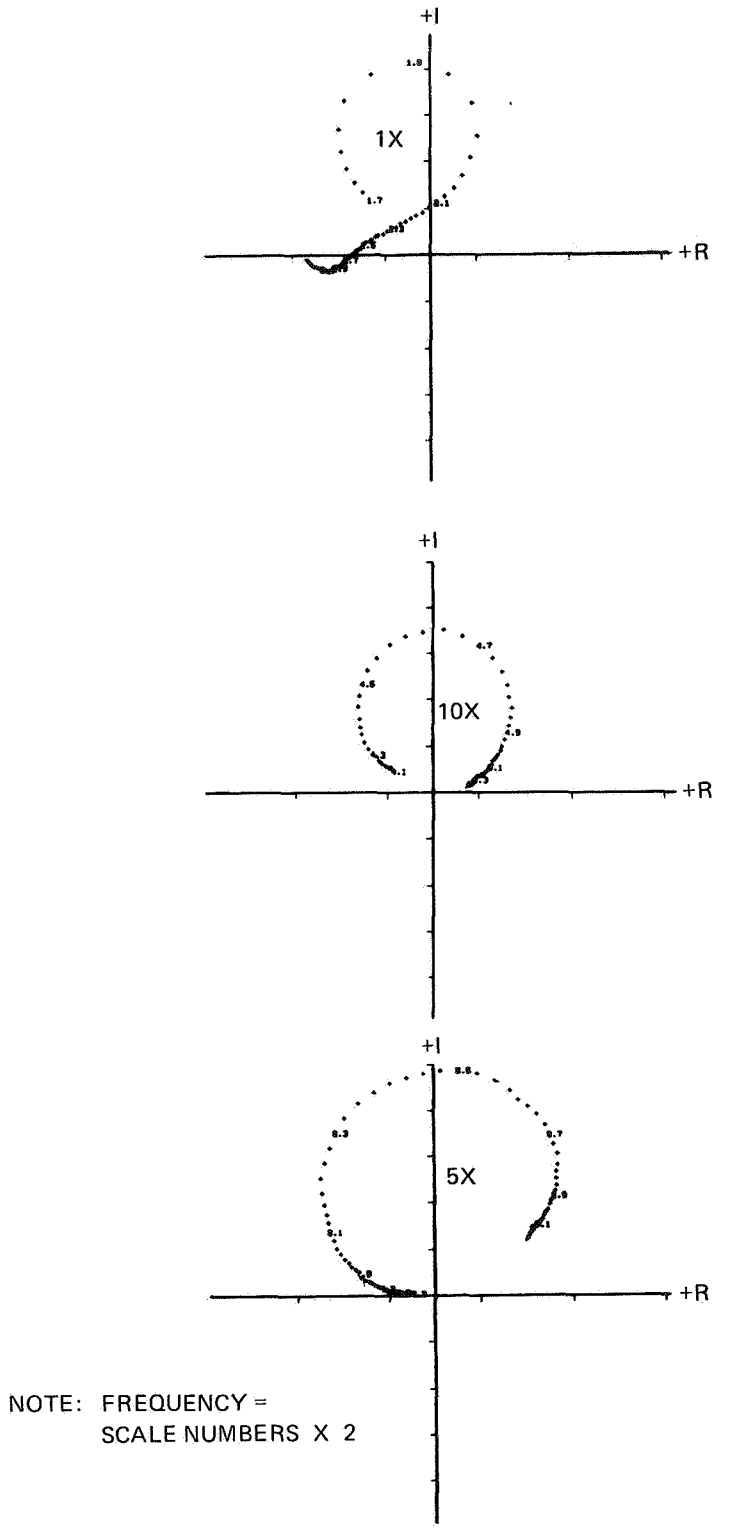

Figure 16.–Typical transfer function plots from transonic empennage model test.

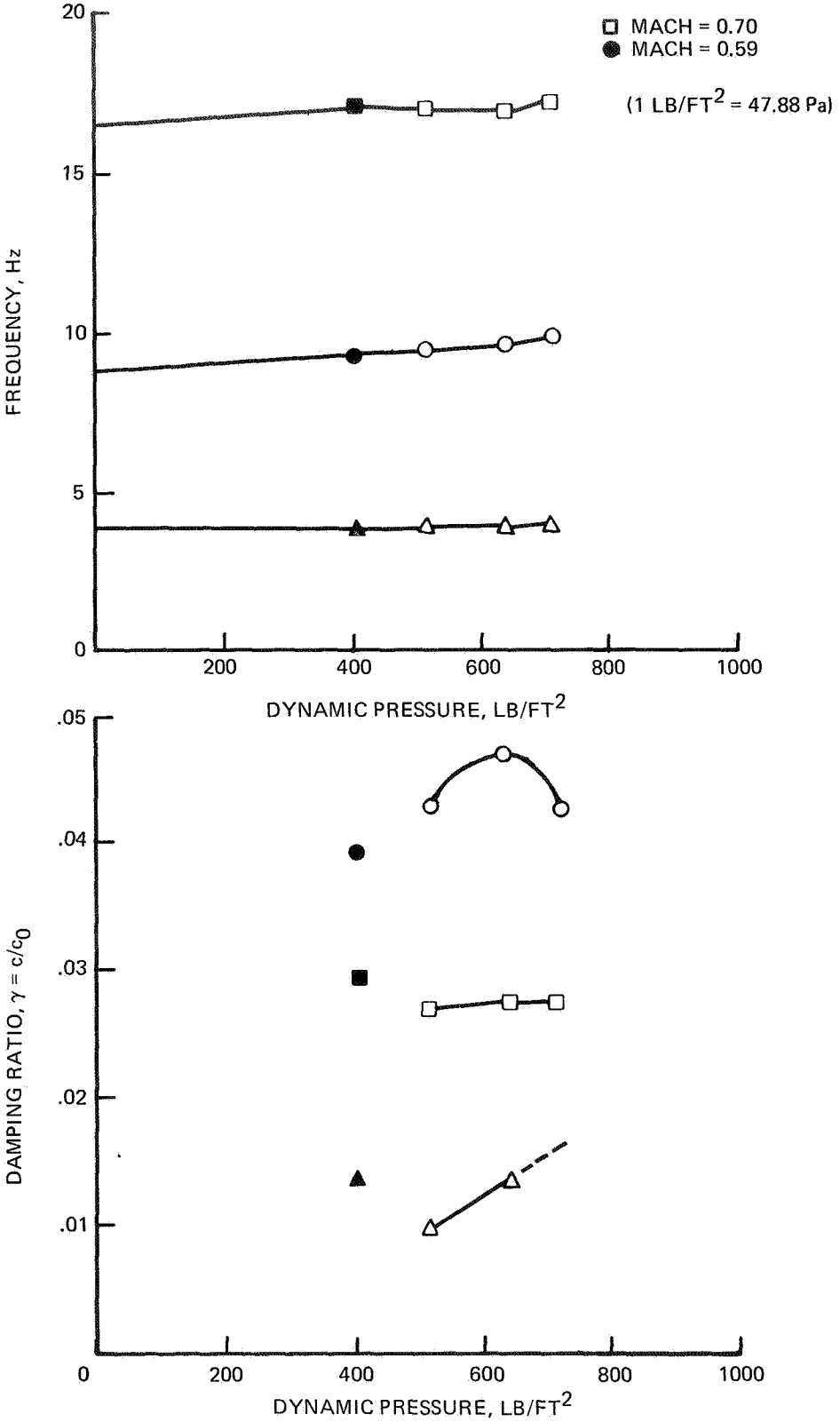

Figure 17.– Dynamic pressure versus damping and frequency.

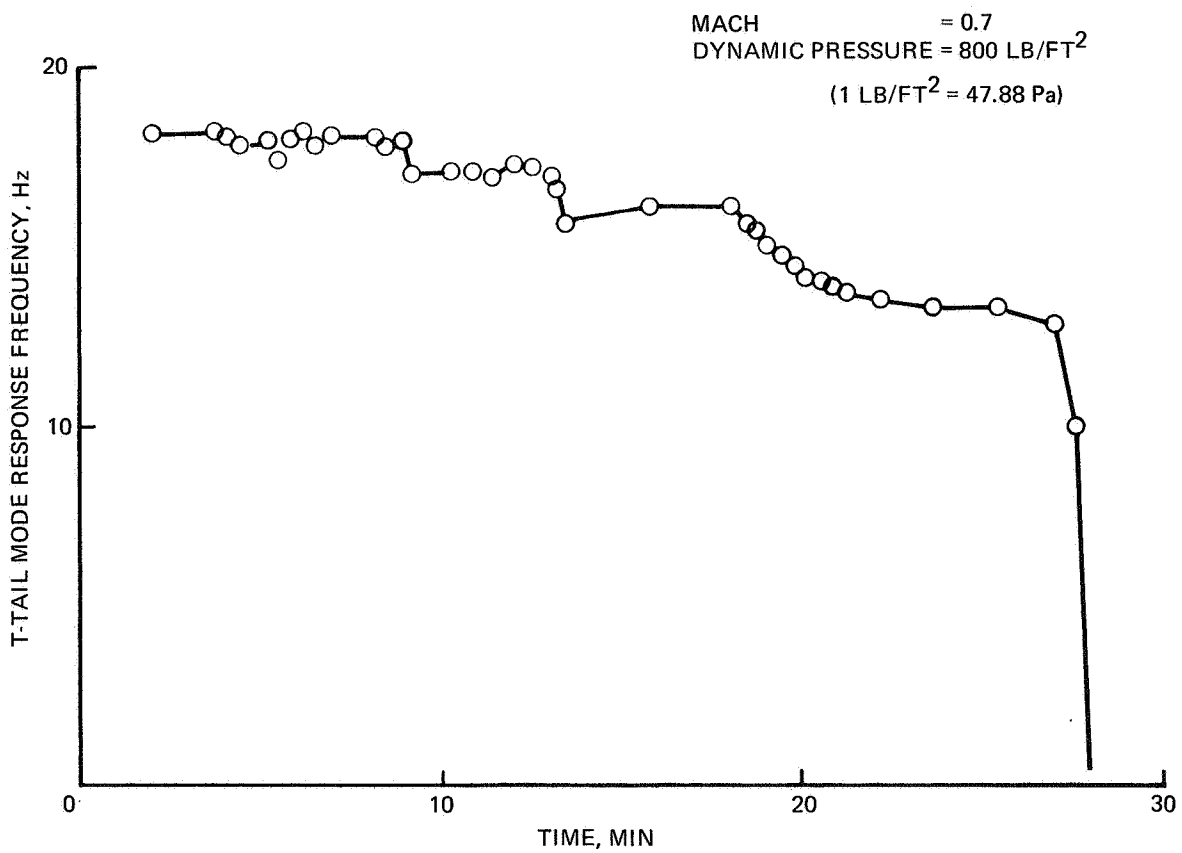

Figure 18.– 727-300 T-tail flutter model.

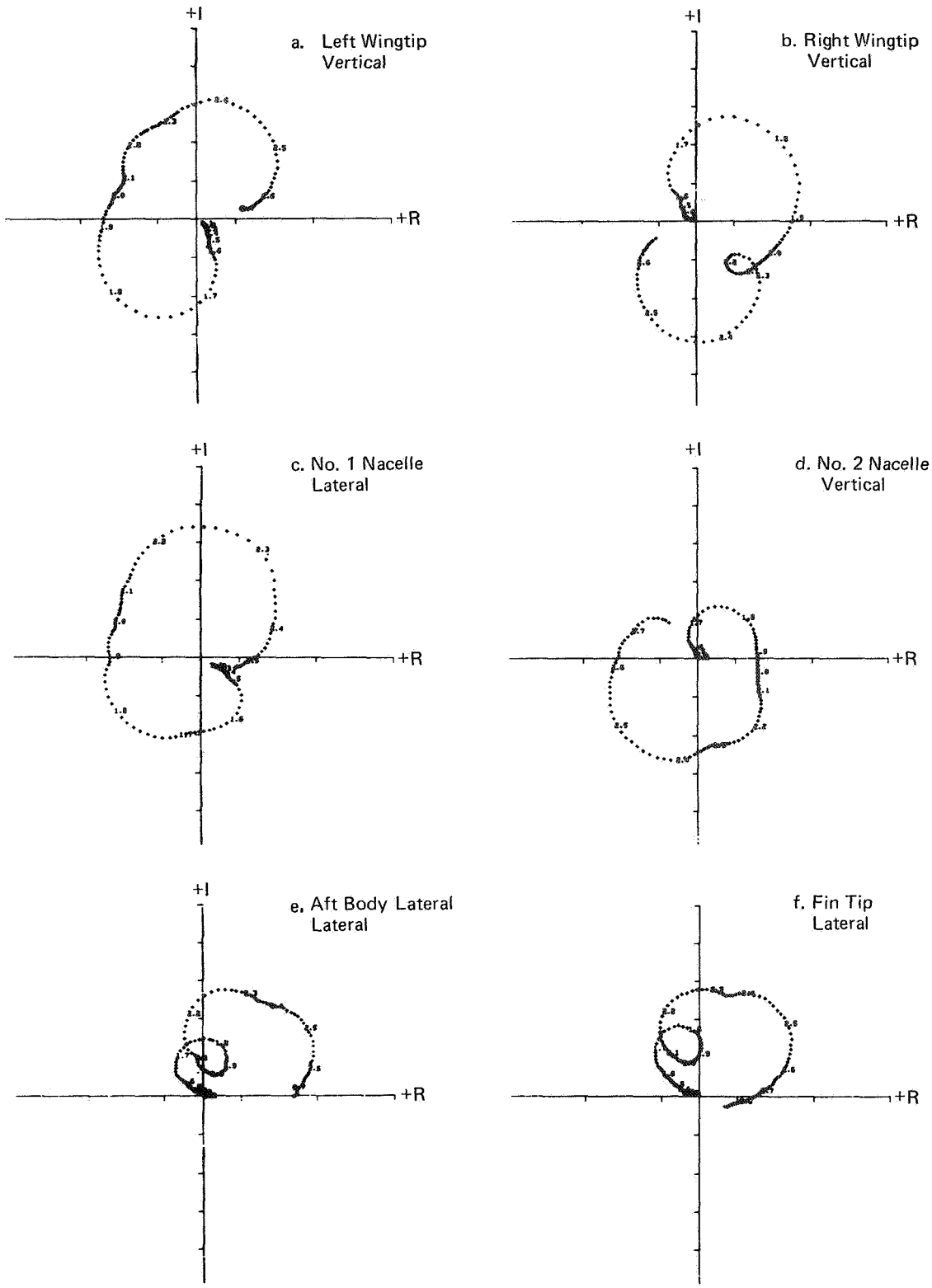

Figure 19.– 747-200 with JT9D-70 engines–Transfer functions relative to rudder excitation.